Cold Test #3
Spartan IR Camera for the SOAR Telescope

Dustin I. Baker & Edwin D. Loh

Department of Physics & Astronomy
Michigan State University, East Lansing, MI 48824

Loh@msu.edu 517 355–9200 x2480

11 January 2007

1 Requirements

Focus Find the focus for one detector for the f/12 and the f/21 channels. Use the 1.523-μm laser, and the H-band filter to make the diffraction size determined by a single wavelength.

Focus across field Check whether the image size for the other 3 detectors matches that of the detector used for focusing.

Detector cosmetics Describe the cosmetic appearance of the four detectors. Are some quadrants usuable? Are there many hot spots?

Flexure Measure flexure for both the f/12 and f/21 channels. Use thermal radiation from the room. Take data in pairs separated by 5°. At the end, repeat the measurement at the starting orientation.

Dark current Use the dark slide.

Detector noise Measure the noise *vs.* amount of light. Use the K-band filter. Use thermal radiation of the room. Cover the window to block solar radiation, which may vary because of clouds. Take pairs of pictures with the same exposure time. We found that the difference between the first pair is larger than subsequent pairs. Take at least 4 pairs.

Detector orientation In the FITS image, the software makes the orientation of all four detectors the same in the sky. Check that this is the case.

Flat field Make a flat field by looking at paper illuminated by an incandescent light. Use a reduced pupil such as the "small pin-hole" pupil stop.

Offset of mechanism positioning between room temperature and 77 K. At the end of the cold test, use “Test Home” to find the reverse limit for all mechanisms. After the instrument is warm, use Test Home again. The difference is the offset of mechanism positioning between room temperature and 77 K.

The antibacklash springs for the mask and big filter wheels have shown wear and loss of positioning. We have not installed the frictionless antibacklash mechanisms. Therefore we do not want to run these wheels needlessly.

2 Installation

Vacuum plug

		Bottom					*Top*		
Pins	*Posn.*	*Contr.*	*Pins*	*Contr.*	*Pins*	*posn.*	*Contr.*	*Pins*	*Contr.*
20	A1	3			30	B2	2		
30	A1	3			20	B2	2		
20	nc		10	3	30	A2	7	10	
30	B1	4			20	A2	7		
20	B1	4			30	nc			
30	nc				20	nc			

Table 1: Cabling. In the table, the cables are oriented as viewed from the air side; the 10-pin cable is to the right of the 20 and 30-pin cables.

Chan.	*Loc.*	*Det. SN*
0	A1	66
1	B1	74
3	B2	92
2	A2	24

Table 2: Channels. Detector 92 is engineering grade; the others are science grade. For Run 1 of Cold Test 3, channels 2 and 3 were swapped.

3 Dark current

Detector 1, Serial #74, has a corner that emits light. The bright corner is in quadrant 1 (counting from 0). See Figure 2. We believe that light is reflected off the curved

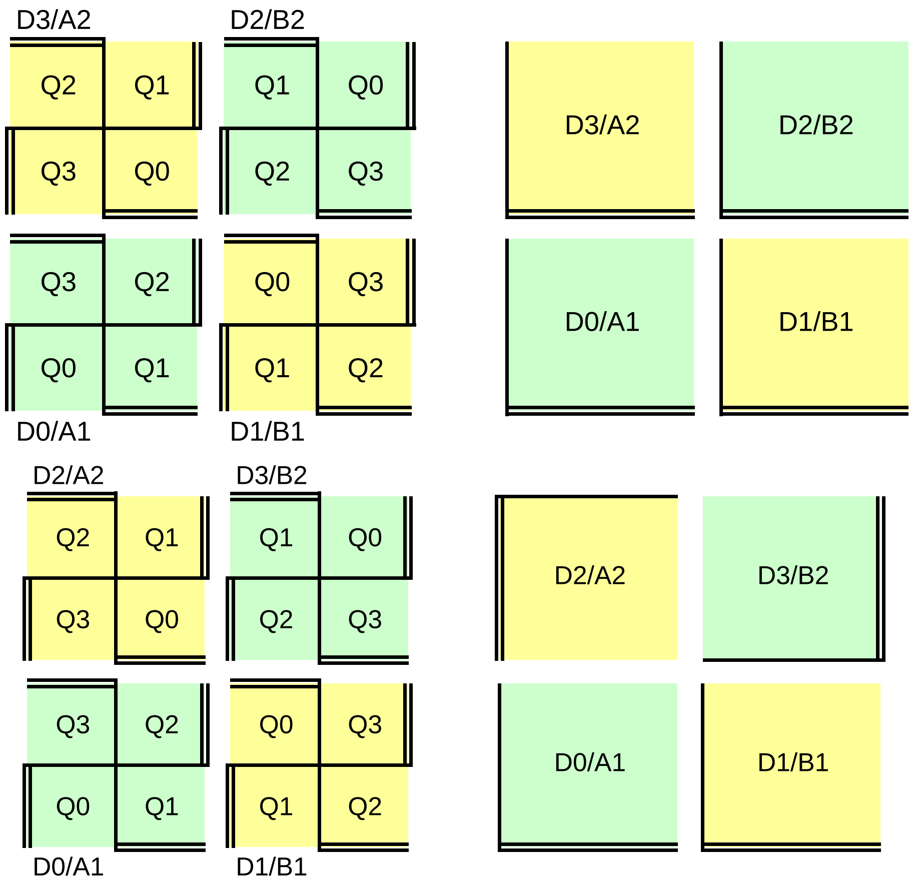

Figure 1: Detector arrangement (top) and arrangement for Run1 (bottom). The double lines is the x-axis, which changes more rapidly in the image file, and the single line is the y-axis.

surface of the field-flattening lens, which is a few mm from the detector, and is focused somewhat onto the opposite quadrant. The horizontal and vertical bands at the bottom and left may be reflection off of the frame that holds the detector. Furthermore, the light appears in the detector at the upper right. The shadow of the pyramid is clear in the image. There is a curved arc for which we have no explanation.

The dark current

SN	*Dark current*		t_{eq}	D/B
	[ADU/s]	[e^-/s]	[s]	
Measured at $T = 89\,\mathrm{K}$				
#66	1.3	5.1	28	0.3
#74	2.4	9.4	15	0.5
Extrapolated to $T = 83\,\mathrm{K}$				
#66	0.2	0.8	180	0.04
#74	0.4	1.4	100	0.08

Table 3: Measured (top two rows) and expected (bottom two rows) dark current D for quadrant 2 of two detectors. To convert between analog-to-digital converter units to electrons, the value of $3.9\,e^-/\mathrm{ADU}$ was used. t_{eq} is the exposure time for which the noise from thermally generated (or otherwise exposure dependent) photoelectrons matches the detector noise. D/B is the ratio of the dark current to the sky background in the darkest broad-band channel, which is the j-band in the high-res channel.

The dark current for detector #66 is a factor of 13 lower than that measured with an engineering-grade detector in Cold Test 2. For detector #74, the factor is 7. The principal improvement is that we fixed a light leak at the entrance of the detector cable. We added a ruffle made of aluminized PET insulation that is tightly taped to the detector cable. The ruffle blocks thermal radiation from entering the hole in the cryo-optical box meant for the detector cables. In addition, we added a baffle made of black Delrin to block the direct path between the cable entrance and a surface that a detector can see.

The temperature of the cryo-optical box was 4 C higher than that for Cold Test 2, and the temperature of the detector was 6 C warmer when the dark current was measured, because the pressure had risen to 0.5 mTorr. Half of the bolts for the reservoir for liquid nitrogen were inadvertantly not installed.

If the temperature had been 6 C cooler, the dark current would be lower by a factor of 7.

Our thermal model predicted a temperature difference between the 0.5 K between

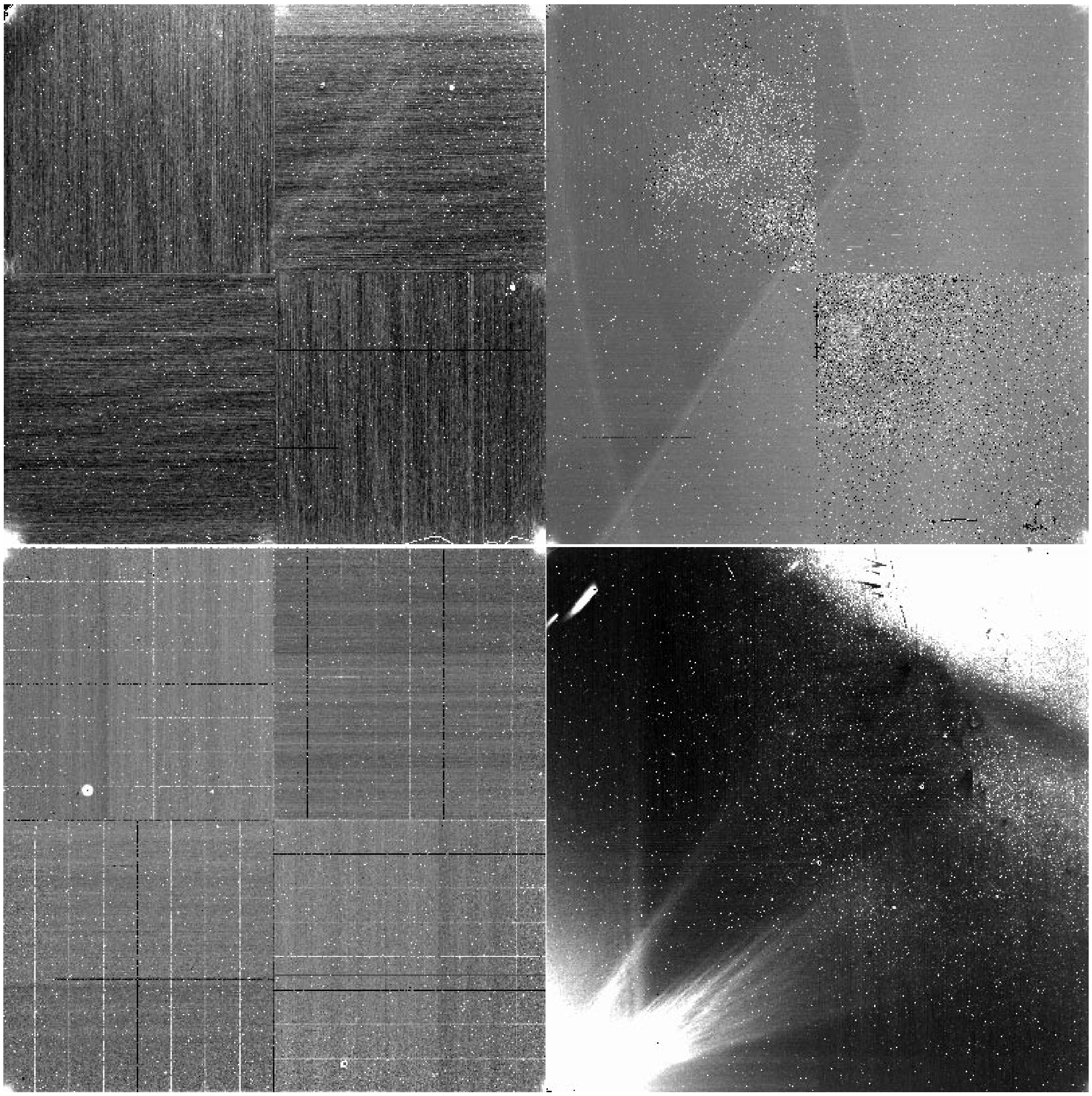

Figure 2: Image taken with a dark slide. The image is printed so that light that reflects off the vicinity of the apex of the pyramid images onto the corners of the figure. To position the 4 sections of the image as if they were pasted onto the surface of the 4 detectors, rotate the four images in this way: For the lower-left detector, rotate the lower-left corner up out of the paper 90° about the axis formed by the lower-right and upper-left corners. For each detector, the outer most corner is raised up.

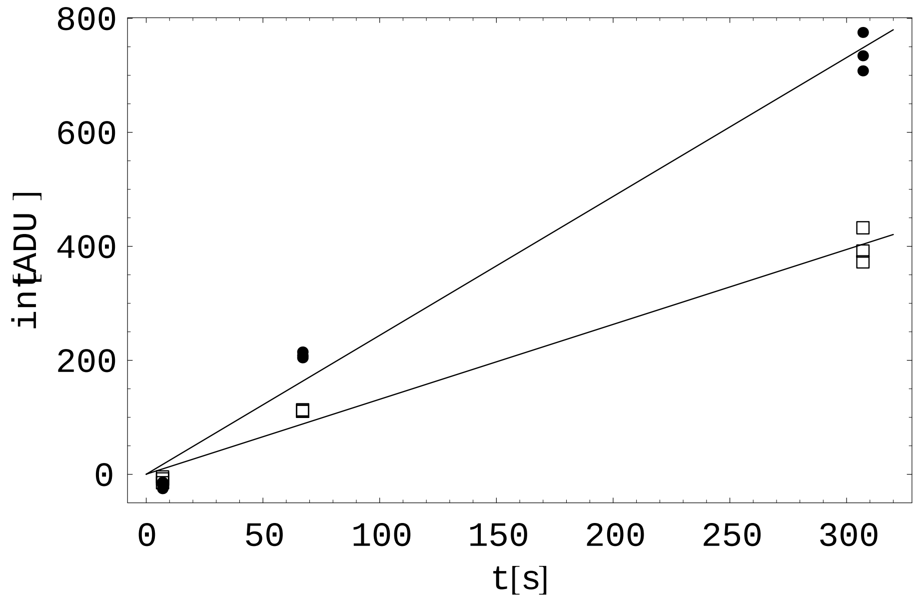

Figure 3: Dark current for quadrant 2 of detectors #66 (box) and #74 (points).

the detector and the cryo-optical box (COB), whereas the measured difference is 2 K. The temperature of the detector is 83 K, and the temperature of the COB is 81 K. The thermal model does not account for the thermal resistance of bolted contacts. The bolted contacts are between a copper strap and a copper button, between a copper strap and an aluminum leg, between a 6061 aluminum leg and the 6061 aluminum spine, and between the aluminum spine and COB.

3.0.1 Use with narrow-band filters

Cássio Leandro of the Universidade do Vale do Paraíba (UNIVAP) plans to purchase narrow-band filters (Table 4). For the one with the darkest sky, HeI, the sky is a factor of 16 darker than that in the J-band.

With the HeI filter, the dark current matches the sky background.

It would be desirable to lower the dark current for observations with the HeI filter. Two possible ways to reduce the dark current are to pump the nitrogen and to install a long heat strap. The latter requires a considerable amount of work.

Filter	λ*(nm)*	$d\,\lambda$
HeI	1083	10
[FeII]	1644	15
Cont.1	2045	30
HeI/CIV	2070	30
H2	2121	20
Cont.2	2140	30
Brgamma	2161	20
Cont.3	2210	30
CO	2325	70

Table 4: Tentative list of narrow-band filters